

LETTER TO THE EDITOR

Discovery of HCCCH₂CCH in TMC-1 with the QUIJOTE line survey[★]

R. Fuentetaja¹, M. Agúndez¹, C. Cabezas¹, B. Tercero^{2,3}, N. Marcelino^{2,3}, J. R. Pardo¹, P. de Vicente², J. Cernicharo¹

¹ Dept. de Astrofísica Molecular, Instituto de Física Fundamental (IFF-CSIC), C/ Serrano 121, 28006 Madrid, Spain.
e-mail: r.fuentetaja@csic.es, jose.cernicharo@csic.es

² Centro de Desarrollos Tecnológicos, Observatorio de Yebes (IGN), 19141 Yebes, Guadalajara, Spain.

³ Observatorio Astronómico Nacional (OAN, IGN), C/ Alfonso XII, 3, 28014, Madrid, Spain.

Received; accepted

ABSTRACT

We present the first detection in space of 1,4-pentadiyne. It has been found towards TMC-1 with the QUIJOTE line survey in the 31-50 GHz range. We observed a total of 17 transitions with $J = 2$ up to 13 and $K_a = 0, 1$ and 2. The observed transitions allowed us to derive a rotational temperature of 9.5 ± 0.5 K and a column density of $(5.0 \pm 0.5) \times 10^{12}$ cm⁻². This molecule was the last non-cyclic isomer of the C₅H₄ family that could be detected via radio astronomy. A computational chemistry study was performed to determine the energies of the five most stable isomers. The isomer (*c*-C₃H₃CCH) has a considerably higher energy than the others, and it has not yet been detected. To better understand the chemical reactions involving these species, we compared the ethynyl and cyano derivatives. The observed abundances of these species are in good agreement with the branching ratios of the formation reactions studied with our chemical model of TMC-1.

Key words. molecular data — line: identification — ISM: molecules — ISM: individual (TMC-1) — astrochemistry

1. Introduction

Studies of the TMC-1 dark cloud have greatly improved our understanding of the chemistry of the interstellar medium. Its carbon-rich composition allows the formation of a large variety of species. A large number of new molecules have been detected in recent years with the Yebes 40m radio telescope via the QUIJOTE¹ line survey (Cernicharo et al. 2021a) and with the Green Bank 100m telescope via the GOTHAM² line survey (McGuire et al. 2018). Recent discoveries include several cyclic molecules, such as benzyne, cyclopentadiene, indene, ortho-benzyne, and fulvenallene (Cernicharo et al. 2021a,b, 2022). Other cycles detected in TMC-1 are the cyano and ethynyl derivatives of cyclopentadiene (McCarthy et al. 2021; Lee et al. 2021; Cernicharo et al. 2021c) and benzene (Loru et al. 2023; McGuire et al. 2018), and cyano derivatives of naphthalene and indene (McGuire et al. 2021; Sita et al. 2022). Among the long carbon chains, molecules such as vinyl acetylene (Cernicharo et al. 2021d), allenyl acetylene (Cernicharo et al. 2021e), butadiynylallene (Fuentetaja et al. 2022a), ethynylbutatrienylidene (Fuentetaja et al. 2022b), propargyl cation (Silva et al. 2023), and propargyl radical (Agúndez et al. 2021), one of the most abundant radicals found, have been discovered in TMC-1. The study of this source is of extreme importance for the correct understanding of chemical processes in the interstellar medium. The results obtained with these surveys also require an improvement of the chemical networks

[★] Based on observations carried out with the Yebes 40m telescope (projects 19A003, 20A014, 20D023, 21A011, 21D005, and 23A024). The 40m radio telescope at Yebes Observatory is operated by the Spanish Geographic Institute (IGN, Ministerio de Transportes, Movilidad y Agenda Urbana).

¹ Q-band Ultrasensitive Inspection Journey to the Obscure TMC-1 Environment

² GBT Observations of TMC-1: Hunting Aromatic Molecules

as several of these molecules are not predicted by the current state-of-the-art chemical models.

Pure hydrocarbons have a crucial role in dark cloud reactions. Their weak rotational transitions, due to the low dipole moment, have complicated their study. However, thanks to the high sensitivity of the QUIJOTE data, we have been able to detect a large number of them, which will provide a census of pure hydrocarbons in TMC-1. The study of ethynyl and cyanide derivatives is of considerable importance as they allow us to follow the different chemical paths to producing them from the same precursor via reactions involving CCH and CN radicals.

In this Letter we report the detection of HCCCH₂CCH, with a total of 18 lines detected with a S/N greater than 3σ in the frequency range 31-50 GHz due to the high sensitivity of the survey. We also report an analysis of the five lowest-energy isomers with a non-zero dipole moment of the C₅H₄ family via a computational study, and we compare the abundance ratios of the detected species with their cyano derivative.

2. Observations

The data utilized in this study are part of the QUIJOTE spectral line survey of TMC-1 in the Q band, which was conducted with the Yebes 40m telescope at the position $\alpha_{J2000} = 4^{\text{h}}41^{\text{m}}41.9^{\text{s}}$ and $\delta_{J2000} = +25^{\circ}41'27.0''$. The receiver, developed under the Nanocosmos project, consists of two cold high-electron mobility transistor amplifiers that cover the 31.0–50.3 GHz band with horizontal and vertical polarizations. The backends are $2 \times 8 \times 2.5$ GHz fast Fourier transform spectrometers with a spectral resolution of 38 kHz, providing the whole coverage of the Q band in both polarizations. A description of the telescope, receivers, and backends is given by Tercero et al. (2021).

The QUIJOTE line survey was performed in multiple observing runs, and frequency-switching observing mode with a

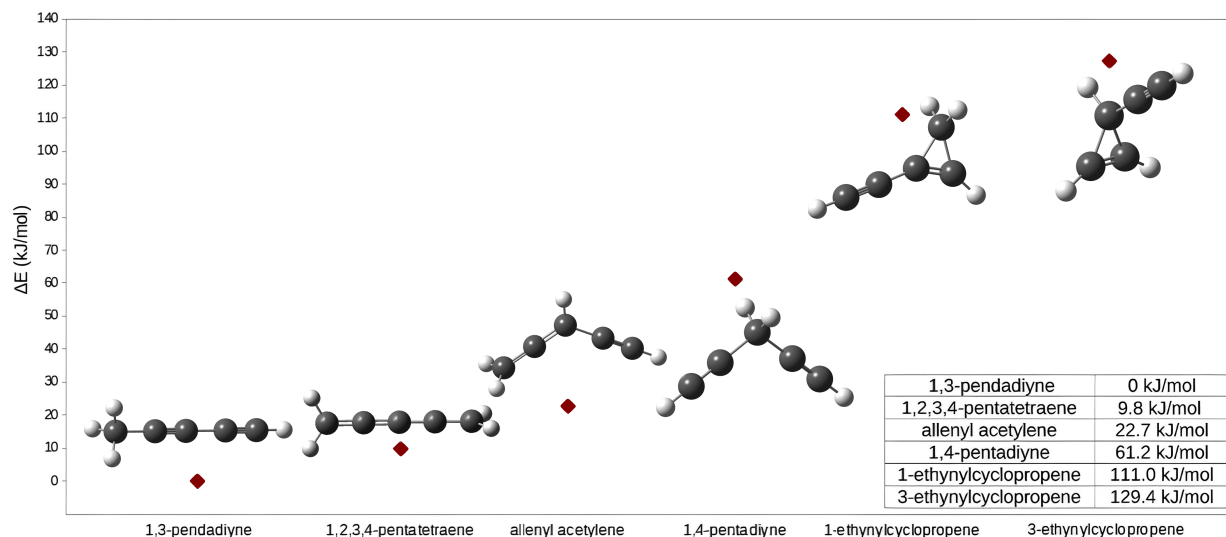


Fig. 1. Relative energy of C_5H_4 isomers calculated at DFT(B3LYP)/cc-pVTZ.

frequency throw of 8 and 10 MHz was used for all observations. The total observing time on the source for data taken with frequency throws of 8 MHz and 10 MHz (465 and 737 hours, respectively) was 1202 hours by November 2023. The noise level ranged from 0.09 mK at 32 GHz to 0.25 mK at 49.5 GHz, which is more than 50 times better than that of previous line surveys of TMC-1 in the Q band (Kaifu et al. 2004). Different local oscillator frequencies were used for each frequency throw to remove any possible sideband effects in the down conversion chain. A detailed account of the QUIJOTE line survey is presented in Cernicharo et al. (2021a).

The main beam efficiency varied from 0.66 at 32 GHz to 0.49 at 50 GHz (Tercero et al. 2021). The telescope beam size is 54.4'' and 36.4'' at 31 and 50 GHz, respectively. The intensity scale utilized in this study was antenna temperature (T_A^*), calibrated using two absorbers at different temperatures, and the atmospheric transmission model (Cernicharo 1985; Pardo et al. 2001). Calibration uncertainties were adopted to be 10%. All the data were analyzed with the GILDAS package³.

3. Results

The C_5H_4 family has a large number of possible isomers. For the search for new isomers, Lattalais et al. (2009, 2010) proposed the principle of minimum energy as a method for obtaining new candidates, since most of the isomers detected are those of minimum energy. For this purpose, we performed geometry optimization calculations to obtain the most stable conformations using the Gaussian16 program package (Frisch et al. 2016) and the B3LYP (Lee et al. 1988) hybrid density functional with the Dunning's correlation consistent polarized valence triple- ζ (cc-pVTZ) (Woon & Dunning 1995). The results are shown in Fig. 1 as a function of the energy difference (including zero-point energy) of the most stable isomer, CH_3C_4H . All the lower-energy molecules have already been detected (except 1,2,3,4-pentatetraene because it has no dipole moment), leaving 1-ethynylcyclopropene as the next candidate to be discovered. Kenny et al. (2001) performed theoretical calculations at different levels for several of these isomers. The values they obtained with the B3LYP functional and the DZP basis sets are quite similar to those derived for this work. The difference between the

data derived by Kenny et al. (2001) and our estimates are 8.4 kJ mol⁻¹ for the two lowest-energy isomers and 7.6 kJ mol⁻¹ for 3-ethynylcyclopropene. However, there is a significant difference between our calculations of the coupled cluster, with differences amounting to 33.5 kJ mol⁻¹ and 16.8 kJ mol⁻¹, respectively.

Methyldiacetylene (CH_3C_4H) was the first C_5H_4 isomer detected in the interstellar medium (MacLeod et al. 1984; Walmley et al. 1984). The next detected isomer ($CH_2CCHCCH$) has an energy 22.7 kJ mol⁻¹ higher than the more stable species and was discovered by Cernicharo et al. (2021f). The species $HCCCH_2CCH$ is the only remaining non-cyclic isomer that can be detected, because the isomer $H_2CCCCCH_2$ is non-polar and therefore has no rotational lines. There are two additional cyclic isomers, which have a significantly higher energy with respect to the non-cyclic ones due to the presence of a cycle of three carbon atoms; this increases their energy relative to the other isomers. No spectroscopic information is available for these two isomers.

The line identification was achieved using the MADEX (Cernicharo 2012) and CDMS (Müller et al. 2005) catalogues. Rotational spectroscopy and the dipole moment ($\mu_b = 0.516D$) for this species were measured in the laboratory by Kuczkowski et al. (1981).

We detected a total of 18 lines within the Q band, with peak intensities ranging from 1.17 mk to 0.41 mK, corresponding to the transitions from $J = 2$ to $J = 13$, with $K_a = 0, 1$, and 2. The molecule has ortho and para species, so the spin statistic (5/3 for K_a odd/even) was included in the calculations. The derived line parameters for the molecules studied in this work were obtained by fitting a Gaussian line profile to the observed data (see Table 1). A window of ± 15 km s⁻¹ around the v_{LSR} of the source was considered for each transition. Results in three of the lines were obtained only with the FSW data with a throw of 8 MHz or 10 MHz, since in the other one the line is affected by the FSW negative features (see notes in Table 1, and Fig. 2). The line $9_{0,9}-8_{1,8}$ is blended with a transition of HC_4N .

To obtain the column density, we used a model line fitting procedure, with the local thermodynamic equilibrium approach for the thin optical lines (see e.g. Cernicharo et al. 2021d). We obtained $N(HCCCH_2CCH) = (5.0 \pm 0.5) \times 10^{12}$ cm⁻² with a rotational temperature of 9.5 ± 0.5 K. We assumed a source of uniform brightness with a diameter of 80'' (Fossé et al. 2001). The H_2 column density for TMC-1 is 10^{22} cm⁻² (Cernicharo

³ <http://www.iram.fr/IRAMFR/GILDAS>

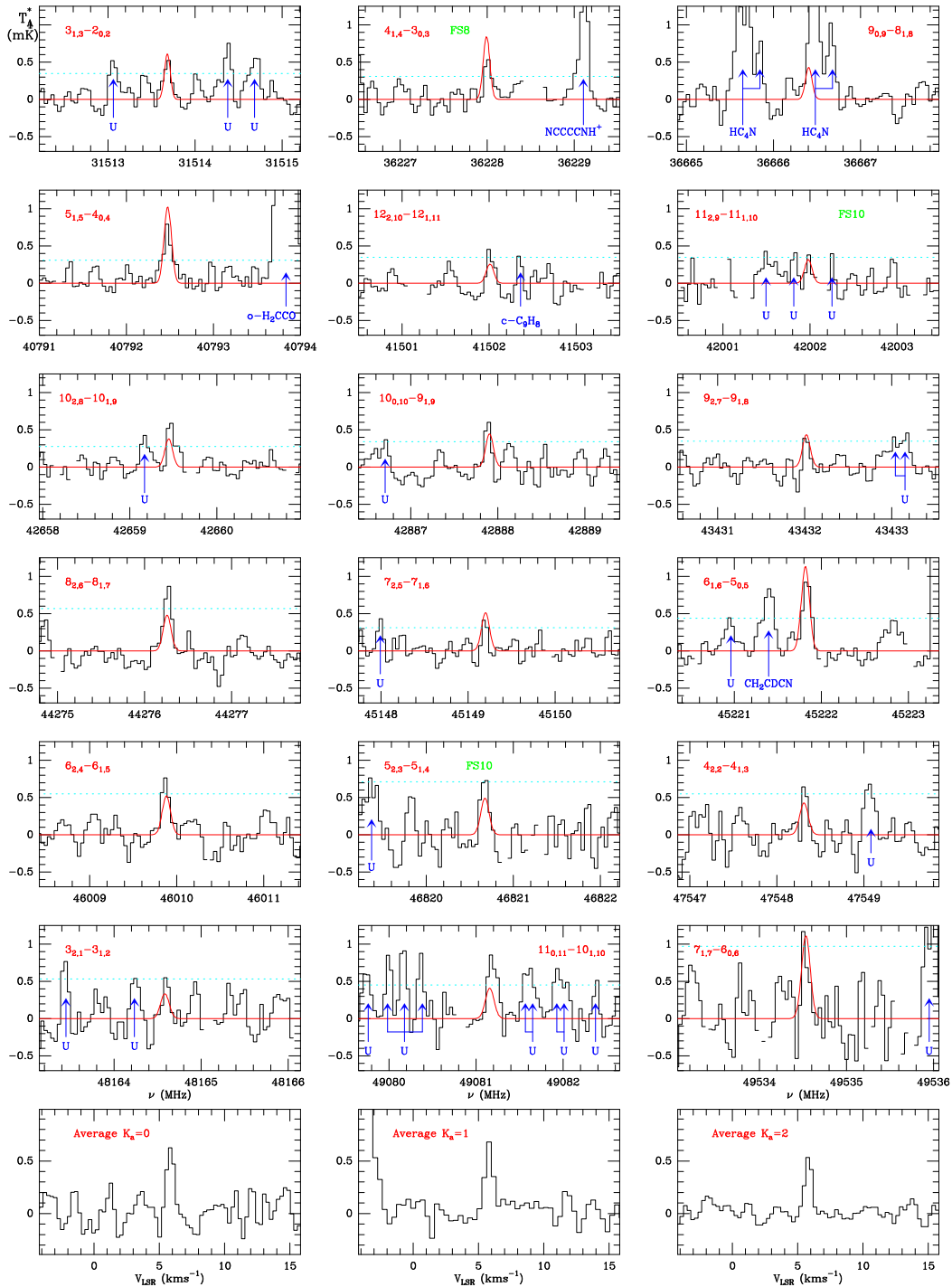


Fig. 2. Selected transitions of HCCCH₂CCH in TMC-1. The abscissa corresponds to the rest frequency of the lines. Frequencies and intensities for all observed lines are given in Table 1. The ordinate is the antenna temperature, corrected for atmospheric and telescope losses, in millikelvins. The quantum numbers of each transition are indicated in the corresponding panel. The red line shows the computed synthetic spectra for this species for $T_{\text{rot}} = 9.5 \pm 0.5$ K and a column density of $(5.0 \pm 0.5) \times 10^{12}$ cm⁻² (see the main text). Blanked channels correspond to negative features produced when folding the frequency-switched data. Green labels indicate the transitions for which only one of the frequency-switching data points has been used (FS10 corresponds to a throw of 10 MHz). The three panels at the bottom show the average of all $K_a=0, 1$, and 2 transitions. The noise level is below 0.1 mK for these stacked spectra. CH₂CDCN is reported in the $6_{16} - 5_{05}$ transition panel. A detailed analysis of the isotopologues of CH₂CHCN will be presented elsewhere (Cernicharo et al., in prep).

& Guélin 1987, Fuentetaja et al. in prep), so the abundance of HCCCH₂CCH is $(5.0 \pm 0.5) \times 10^{-10}$. The predicted synthetic lines for these data are shown in Fig. 2.

Assuming a column density of H₂ of 10^{22} cm⁻² (Cernicharo & Guélin 1987), we see that the detected isomers of C₅H₄ show high abundances, $(\sim 2.5-12) \times 10^{-10}$. It is interesting to

analyse the abundance ratios of these molecules by substituting an ethynyl group for a cyano group (C₄H₃N) because the formation reactions occur through the same precursors, reacting with the CCH and CN radicals, respectively. It is observed that the cyano derivatives have slightly lower column densities (see Table 2). All the abundance ratios obtained for these

Table 1. Observed line parameters of HCCCH₂CCH.

Transition ^a	ν_{rest} ^b (MHz)	$\int T_A^* dv$ ^c (mK km s ⁻¹)	Δv ^d (km s ⁻¹)	T_A^* ^e (mK)	Notes
3 _{1,3} -2 _{0,2}	31513.681±0.015	0.57±0.16	1.07±0.34	0.50±0.11	
4 _{1,4} -3 _{0,3}	36228.011±0.010	0.40±0.14	0.71±0.18	0.54±0.10	A
9 _{0,9} -8 _{1,8}	36666.397				B
5 _{1,5} -4 _{0,4}	40792.476±0.010	0.76±0.13	1.11±0.26	0.65±0.10	
12 _{2,10} -12 _{1,11}	41502.013±0.013	0.27±0.08	0.58±0.18	0.44±0.12	
11 _{2,9} -11 _{1,10}	42001.987±0.019	0.18±0.10	0.43±0.24	0.41±0.12	C
10 _{2,8} -10 _{1,9}	42659.467±0.010	0.39±0.07	0.56±0.11	0.66±0.09	
10 _{0,10} -9 _{1,9}	42887.885±0.010	0.36±0.05	0.50±0.12	0.68±0.10	
9 _{2,7} -9 _{1,8}	43432.014±0.010	0.21±0.09	0.43±0.19	0.50±0.11	
8 _{2,6} -8 _{1,7}	44276.266±0.010	0.67±0.11	0.72±0.14	0.88±0.19	
7 _{2,5} -7 _{1,6}	45149.193±0.010	0.20±0.05	0.38±0.10	0.50±0.10	
6 _{1,6} -5 _{0,5}	45221.835±0.010	0.85±0.13	0.81±0.15	0.98±0.14	
6 _{2,4} -6 _{1,5}	46009.868±0.010	0.60±0.10	0.73±0.15	0.77±0.18	
5 _{2,3} -5 _{1,4}	46820.668±0.010	0.60±0.20	0.69±0.22	0.82±0.27	C
4 _{2,2} -4 _{1,3}	47548.326±0.010	0.35±0.06	0.38±0.13	0.87±0.18	
3 _{2,1} -3 _{1,2}	48164.599±0.020	0.36±0.12	0.57±0.23	0.59±0.19	
11 _{0,11} -10 _{1,10}	49081.189±0.018	0.69±0.19	0.76±0.21	0.85±0.15	
7 _{1,7} -6 _{0,6}	49534.521±0.010	0.72±0.22	0.58±0.19	1.17±0.33	

Notes.

(^a) Quantum numbers are $J'_{K'_a, K'_c} - J_{K_a, K_c}$. (^b) Observed frequency of the transition assuming a local standard of rest velocity of 5.83 km s⁻¹. (^c) Integrated line intensity in mK km s⁻¹. (^d) Linewidth at half intensity derived by fitting a Gaussian function to the observed line profile in km s⁻¹. (^e) Antenna temperature in millikelvins. (^A) Frequency-switching data with a throw of 8 MHz only. Negative feature present in the data with a 10 MHz throw. (^B) This line is blended with a transition of HC₄N. (^C) Frequency-switching data with a throw of 10 MHz only. Negative feature present in the data with a 8 MHz throw.

Table 2. Derived rotational temperatures and column densities for C₅H₄ and C₄H₃N isomers towards TMC-1.

Molecule	T_{rot} (K)	N (cm ⁻²)
HCCCH ₂ CN ^a	4 ± 1	2.8 ± 0.7 × 10 ¹²
CH ₂ CCHCN ^a	5.5 ± 0.3	2.7 ± 0.2 × 10 ¹²
A - CH ₃ C ₃ N ^a	6.7 ± 0.2	9.7 ± 0.3 × 10 ¹¹
E - CH ₃ C ₃ N ^a	8.2 ± 0.6	7.7 ± 0.5 × 10 ¹¹
CH ₂ CCHCCH ^b	7 ± 1	1.2 ± 0.2 × 10 ¹³
A/E - CH ₃ C ₄ H ^b	7.0 ± 0.3	6.5 ± 0.3 × 10 ¹²
HCCCH ₂ CCH	9.5 ± 0.5	5.0 ± 0.5 × 10 ¹²

Notes.

(^a) Values reported by Marcelino et al. (2021)
(^b) Values reported by Cernicharo et al. (2021f)

species are very similar. For the allenyl acetylene and cyano allene (CH₂CCHCCH/CH₂CCHCN), we obtain a value of 4.5, which was also reported by Cernicharo et al. (2021f). For the most abundant isomers (CH₃C₄H/CH₃C₃N), we obtain a value of 3.7. Finally, from the column density obtained in this Letter, the abundance ratio HCCCH₂CCH/HCCCH₂CN = 1.8.

4. Chemical model

To study the chemistry of C₅H₄ isomers in TMC-1, we carried out calculations using a pseudo-time-dependent gas-phase chemical model. The model is based on the model presented by Cernicharo et al. (2021f) and is in line with the detection of CH₂CCHCCH in TMC-1. Briefly, we considered a gas kinetic temperature of 10 K, a volume density of H₂ of 2 × 10⁴ cm⁻³, a visual extinction of 30 mag, a cosmic-ray ionization rate of H₂ of 1.3 × 10⁻¹⁷ s⁻¹, and the so-called low-metal elemental abundances (Agúndez & Wakelam 2013).

The core of the chemical network is based on RATE12 from the UMIST database (McElroy et al. 2013), with some updates

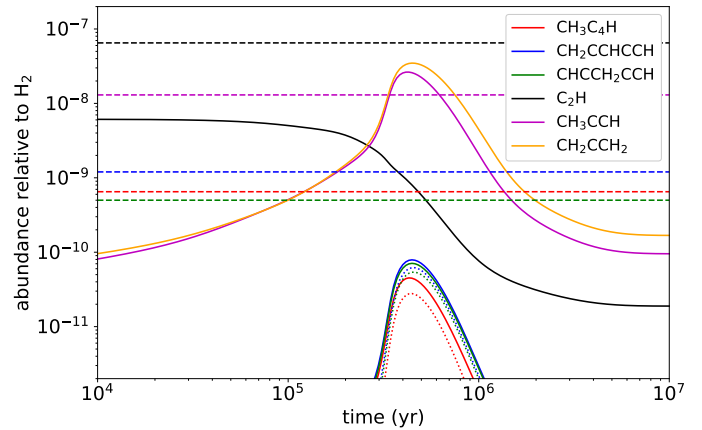
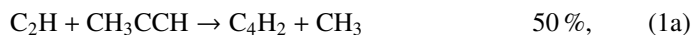


Fig. 3. Fractional abundances of three C₅H₄ isomers calculated with the chemical model as a function of time. Dotted lines correspond to calculated abundances when the dissociative recombination of C₅H₅⁺ is neglected as a source of C₅H₄ isomers. The abundances observed in TMC-1 (from this work and Cernicharo et al. 2022) are indicated by horizontal dashed lines.

(see Marcelino et al. 2021). We included three new C₅H₄ isomers, namely CH₃C₄H, CH₂CCHCCH, and CHCCH₂CCH. The formation and destruction of the three isomers are based on the reactions previously considered for CH₃C₄H, which is the only C₅H₄ isomer considered in the UMIST database. In particular, the three isomers are destroyed by reactions with C neutral atoms with abundant cations, such as C⁺, H⁺, H₃⁺, HCO⁺, and He⁺, and with secondary ultraviolet photons arising from cosmic ray impacts. Among the reactions of formation of CH₃C₄H included in the UMIST database, there is the dissociative recombination of C₅H₅⁺, although there is no evidence as to whether C₅H₄ isomers are produced in this reaction. In the absence of better constraints, we assumed that the three C₅H₄ isomers are produced with equal yields. The UMIST database also includes the reaction between C₂ and propene as a source of CH₃C₄H. This reaction is known to be rapid at low temperatures (Daugey et al. 2008), although the main products are C₅H₅ isomers, rather than C₅H₄ isomers (Dangi et al. 2013). We therefore did not include this reaction as a source of C₅H₄ isomers. The remaining processes of CH₃C₄H formation included in the UMIST database are the reactions of C₂H with methylacetylene and allene. These reactions have been widely studied through experiments and theoretical calculations. First, the reactions were measured to be fast at low temperatures (Hoobler & Leone 1999; Vakhtin et al. 2001; Carty et al. 2001). The rate coefficient measured at 63 K is 2.9 × 10⁻¹⁰ cm³ s⁻¹ for C₂H + CH₃CCH and 3.5 × 10⁻¹⁰ cm³ s⁻¹ for C₂H + CH₂CCH₂ (Carty et al. 2001). The product distribution has also been studied through crossed beams experiments (Kaiser et al. 2001; Zhang et al. 2009), ab initio calculations (Stahl et al. 2001; Jamal & Mebel 2010), and experiments using mass spectrometry and synchrotron photoionization (Goulay et al. 2007, 2011). These studies indicate that the reaction of C₂H with methylacetylene produces diacetylene and the C₅H₄ isomers CH₃C₄H and CH₂CCHCCH (Goulay et al. 2007; Jamal & Mebel 2010), while the reaction of C₂H with allene produces the C₅H₄ isomers CH₂CCHCCH and CHCCH₂CCH (Goulay et al. 2007; Zhang et al. 2009; Jamal & Mebel 2010). We thus in-

cluded the reactions



where the branching ratios are based on the aforementioned studies. We adopted the rate coefficients measured at 63 K (Carty et al. 2001). We note that the reaction of C₂H with allene has also been found to yield the non-polar C₅H₄ isomer CH₂CCCCH₂, although the yield should be lower than 10% (Goulay et al. 2011). The C₅H₄ isomer ethynylallene (CH₂CCHCCH) is expected to be the major product of the reaction CH + CH₂CHCCH (He et al. 2022), and thus we included this reaction with a rate coefficient of $3 \times 10^{-10} \text{ cm}^3 \text{ s}^{-1}$, which is of the order of the values measured at low temperatures for many other rapid neutral-neutral reactions.

The resulting abundances of the three isomers of C₅H₄ detected in TMC-1 are shown in Fig. 3. The peak abundances of the three C₅H₄ isomers, reached at a time of $(4-5) \times 10^5 \text{ yr}$, are very similar. At these times, the main reactions of formation of the three C₅H₄ isomers are the reactions of C₂H with CH₃CCH and CH₂CCH₂, together with the dissociative recombination of C₅H₅⁺. The dotted lines in Fig. 4 show the calculated abundances when the latter pathway, which is more speculative, is neglected. Since the precursors methylacetylene and allene are predicted to have similar abundances (allene being slightly more abundant than methylacetylene; see Fig. 3) and since the branching ratios yielding the three isomers in reactions (1) and (2) are also similar, the resulting abundances are very close. This is in agreement with the fact that observed abundances are also quite similar. The main discrepancy between the model and the observations is that the calculated abundances lie one order of magnitude below the observed ones. In Fig. 3 we also plot the abundance of the precursors involved in reactions (1) and (2). While the calculated abundance of CH₃CCH is of the order of the observed value, the model underestimates the observed abundance in the case of C₂H, which translates into the underestimation of the abundances of the three C₅H₄ isomers. The lesson learnt from the chemical model is that the reactions of C₂H with methylacetylene and allene are the main sources of C₅H₄ isomers in TMC-1. The underestimation of the abundance of HCCCH₂CCH is likely due to an underestimation of the abundance of the precursor C₂H. Alternatively, there could be other formation routes missing in the chemical model.

5. Conclusions

We report the first detection of HCCCH₂CCH in TMC-1. We observed a total of 18 rotational transitions, from $J = 2$ to 13 and $K_a \leq 2$, using the Yebes 40m telescope. The rotational temperature obtained is $9.5 \pm 0.5 \text{ K}$ and the derived column densities are $(5.0 \pm 0.5) \times 10^{12} \text{ cm}^{-2}$. We carried out a comparison of the energies of their five most stable isomers using theoretical calculations, and we obtained different abundance ratios with their cyano derivatives in order to contribute to the understanding of the chemical processes involving these species. The abundances of the three isomers are very similar, which is in agreement with

the branching yielding ratios of the reactions of C₂H with methylacetylene and allene, although the model underestimates their values.

Acknowledgements. We thank Ministerio de Ciencia e Innovación of Spain (MCIU) for funding support through projects PID2019-106110GB-I00, PID2019-107115GB-C21 / AEI / 10.13039/501100011033, and PID2022-137980NB-I00. We also thank ERC for funding through grant ERC-2013-Syg-610256-NANOCOSMOS. M.A. thanks MCIU for grant RyC-2014-16277.

References

- Agúndez, M. & Wakelam, V. 2013, *Chem. Rev.*, 113, 8710
 Agúndez, M., Cabezas, C., Tercero, B., et al. 2021, *A&A*, 647, L10
 Carty, D., Le Page, V., Sims, I. R., & Smith, I. W. M. 2001, *Chem. Phys. Lett.*, 344, 310
 Cernicharo, J. 1985, Internal IRAM report (Granada: IRAM)
 Cernicharo, J. & Guélin, M. 1987, *A&A*, 176, 299
 Cernicharo, J., 2012, in *ECLA 2011: Proc. of the European Conference on Laboratory Astrophysics*, EAS Publications Series, 2012, Ed.: C. Stehl, C. Joblin, & L. d'Hendecourt (Cambridge: Cambridge Univ. Press), 251; https://nanocosmos.iff.csic.es/?page_id=1619
 Cernicharo, J., Agúndez, M., Kaiser, R., et al. 2021a, *A&A*, 652, L9
 Cernicharo, J., Agúndez, M., Cabezas, C., et al. 2021b, *A&A*, 647, L2
 Cernicharo, J., Agúndez, M., Cabezas, C., et al. 2021c, *A&A*, 649, L15
 Cernicharo, J., Cabezas, C., Endo, Y., et al. 2021d, *A&A*, 646, L3
 Cernicharo, J., Cabezas, C., Agúndez, M., et al. 2021e, *A&A*, 648, L3
 Cernicharo, J., Cabezas, C., Agúndez, M., et al. 2021f, *A&A*, 647, L3
 Cernicharo, J., Fuentetaja, R., Agúndez, M., et al. 2022, *A&A*, 663, L9
 Dangi, B. B., Maity, S., Kaiser, R. I., et al. 2013, *Journal of Physical Chemistry A*, 117, 11783
 Daugey, N., Caubet, P., Bergeat, A., et al. 2008, *Phys. Chem. Chem. Phys.*, 10, 729
 Frisch, M. J., Trucks, G. W., Schlegel, H. B., et al. 2016, *Gaussian 16 Revision A.03*
 Fossé, D., Cernicharo, J., Gerin, M., Cox, P. 2001, *ApJ*, 552, 168
 Fuentetaja, R., Cabezas, C., Agúndez, M., et al. 2022a, *A&A*, 663, L3
 Fuentetaja, R., Agúndez, M., Cabezas, C., et al. 2022b, *A&A*, 667, L4
 Goulay, F., Osborn, D. L., Taatjes, C. A., et al. 2007, *Phys. Chem. Chem. Phys.*, 9, 4291
 Goulay, F., Soorkia, S., Meloni, G., et al. 2011, *Phys. Chem. Chem. Phys.*, 13, 20820
 He, C., Yang, Z., Doddipatla, S., et al. 2022, *Phys. Chem. Chem. Phys.*, 24, 26499
 Hoobler, R. J. & Leone, S. R. 1999, *J. Phys. Chem. A*, 103, 1342
 Jamal, A. & Mebel, A. M. 2010, *Phys. Chem. Chem. Phys.*, 12, 2606
 Kaifu, N., Ohishi, M., Kawaguchi, K., et al. 2004, *PASJ*, 56, 69
 Kaiser, R. I., Chiong, C. C., Asvany, O., et al. 2001, *Chem. Phys.*, 114, 3488
 Kenny, J. P., Krueger, K. M., Rienstra-Kiracofe, J. C., et al. 2001, *Journal of Physical Chemistry A*, 105, 7745
 Kuczkowski, R. L., Lovas, F. J., Suenram, R. D., et al. 1981, *Journal of Molecular Structure*, 72, 143
 Lattelais, M., Puzat, F., Ellinger, Y., et al. 2009, *ApJ*, 696, L133
 Lattelais, M., Puzat, F., Ellinger, Y., et al. 2010, *A&A*, 519, A30
 Lee, C., Yang, W., & Parr, R. G. 1988, *Phys. Rev. B*, 37, 785
 Lee, K. L. K., Changala, P. B., Loomis, R. A., et al. 2021, *ApJ*, 910, L2
 Loru, D., Cabezas, C., Cernicharo, J., et al. 2023, *A&A*, 677, A166
 MacLeod, J. M., Avery, L. W., & Broten, N. W. 1984, *ApJ*, 282, L89
 Marcelino, N., Tercero, B., Agúndez, M., et al. 2021, *A&A*, 646, L9
 McCarthy, M. C., Lee, K. L. K., Loomis, R. A., et al. 2021, *Nature Astronomy*, 5, 176
 McElroy, D., Walsh, C., Markwick, A. J., et al. 2013, *A&A*, 550, A36
 McGuire, B. A., Burkhardt, A. M., Kalenskii, S., et al. 2018, *Science*, 359, 202
 McGuire, B. A., Loomis, R. A., Burkhardt, A. M., et al. 2021, *Science*, 371, 1265
 Müller, H.S.P., Schlöder, F., Stutzki, J., Winnewisser, G. 2005, *J. Mol. Struct.*, 742, 215
 Lee, W. Yang and R. G. Parr, *Phys. Rev. B: Condens. Matter Mater. Phys.*, 1988, 37, 785–789.
 Pardo, J. R., Cernicharo, J., Serabyn, E. 2001, *IEEE Trans. Antennas and Propagation*, 49, 12
 Silva, W. G. D. P., Cernicharo, J., Schlemmer, S., et al. 2023, *A&A*, 676, L1
 Sita, M. L., Changala, P. B., Xue, C., et al. 2022, *ApJ*, 938, L12
 Stahl, F., von Rahué Schleyer, P., Bettinger, H. F., et al. 2001, *J. Chem. Phys.*, 114, 3476
 Tercero, F., López-Pérez, J. A., Gallego, et al. 2021, *A&A*, 645, A37
 Vakhtin, A. B., Heard, D. E., Smith, I. W. M., & Leone, S. R. 2001, *Chem. Phys. Lett.*, 344, 317
 Walmsley, C. M., Jewell, P. R., Snyder, L. E., et al. 1984, *A&A*, 134, L11
 Woon, D. E. & Dunning, T. H. 1995, *J. Chem. Phys.*, 103, 4572
 Zhang, F., Kim, S., & Kaiser, R. I. 2009, *Phys. Chem. Chem. Phys.*, 11, 4707